Aerosol and Air Quality Research, 20: 477–488, 2020

ISSN: 1680-8584 print / 2071-1409 online
doi: 10.4209/aaqr.2019.10.0546

Effect of Ceria Doping on the Catalytic Activity and SO_2 Resistance of MnO_x/TiO_2 Catalysts for the Selective Catalytic Reduction of NO with NH_3 at Low Temperatures

Qiulin Wang[1,2], Jianjian Zhou[1], Jianchao Zhang[1], Hao Zhu[1], Yuheng Feng[3*], Jing Jin[1,2]

[1] *School of Energy and Power Engineering, University of Shanghai for Science and Technology, Shanghai 200093, China*
[2] *Shanghai Key Laboratory of Multiphase Flow and Heat Transfer in Power Engineering, University of Shanghai for Science and Technology, Shanghai 200093, China*
[3] *Thermal and Environmental Engineering Institute, Tongji University, Shanghai 200092, China*

ABSTRACT

With its industrial applicability and low energy consumption, a process for implementing the NH_3-SCR of NO at low temperatures is urgently needed. In this study, MnO_x-CeO_2/TiO_2 (MnCe/Ti) catalysts doped with different amounts of Ce were prepared and experimentally examined for their NH_3-SCR activity between 100°C and 400°C. Adding a small amount of Ce (at the Ce/Ti mole ratio of 0.05) elevated the exposure of Mn atoms on the catalyst surface, resulting in the highest NH_3-SCR activity occurring between 100°C and 200°C (with a conversion rate of above 98% for the NO at 175°C). Further increasing the Ce content, however, diminished the catalytic performance. Moreover, the NH_3-SCR of NO during oxidization or reduction atmosphere confirmed that oxygen species bound to the exposed Mn atoms were released more easily and the resulting vacancies were more likely to be replenished by O_2 at low temperatures. In addition, incorporating Ce enhanced the SO_2 resistance of the MnCe/Ti, mainly by inhibiting the accumulation of ammonium sulfates and the preferential sulfation of the Ce dopants.

Keywords: MnO_x/TiO_2; Ce modification; Low-temperature SCR; $deNO_x$; SO_2 poisoning.

INTRODUCTION

Nitrogen oxides (NO_x) are one of the main air contaminants from fossil fuel combustion in power plant and vehicles. Selective catalytic reduction (SCR) of NO_x with NH_3 has been proven to be an efficient, reliable and economical post-combustion technology to control NO_x emissions from stationary sources (Andreoli *et al.*, 2015; Jiang *et al.*, 2017; Yao *et al.*, 2017). Nowadays, the vanadium-based catalysts (V_2O_5/TiO_2 or V_2O_5-WO_3/TiO_2) are widely used as commercial catalysts for NH_3-SCR process whereas these catalysts work efficiently in the narrow temperature window of 300–400°C (Chang *et al.*, 2013; Roy *et al.*, 2009; Jiang *et al.*, 2017; Song *et al.*, 2017). Auxiliary devices are normally required for heating the exhaust to achieve high NO_x conversions. Such approach generally consumes additional energy and increases the greenhouse gases emissions (Sultana *et al.*, 2012).

As an alternative to VO_x, MnO_x catalysts have attracted more interests due to their higher catalytic activities for NH_3-SCR of NO_x (Qi *et al.*, 2003, 2004; Wang *et al.*, 2012; Fan *et al.*, 2018), decomposition of volatile organic compounds (VOCs) (Tian *et al.*, 2010) and persistent organic pollutants (POPs) (Yang *et al.*, 2013) at low temperatures (< 200°C). MnO_x generally owns multiple valences ($Mn^{4+}/Mn^{3+}/Mn^{2+}$) and contains various kinds of labile oxygen, which are necessary to accomplish a catalytic redox cycle and significant factors for its excellent low-temperature catalytic activity (Yang *et al.*, 2013; Yu *et al.*, 2017). However, MnO_x catalysts are highly susceptible to acid gases (e.g., HCl and SO_2) in exhausted gas especially at low temperatures, which restricts their wide application (Wang *et al.*, 2015; Tang *et al.*, 2007). Cerium oxide (CeO_2) is frequently selected as a promoter (Long *et al.*, 2000; Qiu *et al.*, 2015) or an active component (Ma *et al.*, 2015) of SCR catalysts for the unique redox couple Ce^{4+}/Ce^{3+}, which allows a flexible shift between CeO_2 and Ce_2O_3 and promise the catalyst with great oxygen storage/release capacity under oxidizing or reducing conditions (Li *et al.*, 2014; Jiang *et al.*, 2018). To further improve the thermal stability, anti-poisoning ability and SCR activity of MnO_x, many researchers modified MnO_x catalyst with Ce (Wu *et al.*, 2009; Lee *et al.*, 2012; Jin *et al.*, 2014; Li *et al.*,

* Corresponding author.
Tel.: +86 21 65985009; Fax: +86 21 65982786
E-mail address: fengyh@tongji.edu.cn

2014; Andreoli *et al.*, 2015; Kwon *et al.*, 2015; Tang *et al.*, 2016). Expected results have been obtained that modification of MnO_x with Ce greatly improves the catalytic performance by coupling the variable oxidation states of MnO_x with the fast redox cycle of CeO_2 (Lee *et al.*, 2012; Andreoli *et al.*, 2015). Besides, TiO_2 is commonly used as a catalyst supporter due to its large surface area, high thermal stability, strong mechanical strength and high sulfur resistance (Ettireddy *et al.*, 2007). Therefore, TiO_2-supported Mn-Ce mixed oxide catalysts have been intensely studied with extraordinarily high activity for NO_x removal (Lee *et al.*, 2012; Nam *et al.*, 2017).

In this work, MnCe/Ti catalysts with different doping contents of Ce were prepared by sol-gel method. The relationship between the catalyst property and activity was investigated with the help of activity evaluation combined with catalytic characterizations. Moreover, the deactivation and regeneration of the catalysts without or with O_2 were carried out to reveal the oxygen storage/release capability of the catalysts. Furthermore, the SO_2 resistance of MnCe/Ti catalysts was also evaluated. This study provides basic data and guidelines for future development of low-temperature SCR catalyst.

MATERIALS AND METHODS

Catalyst Preparation and Characterization

The tested MnCe/Ti catalysts were prepared by sol-gel method. Firstly, tetrabutyl titanate (0.2 mol), acetic acid (30 mL) were mixed in ethanol (30 mL) and the mixture was stirred and then dripped into the mixed solution of manganese nitrate, cerium nitrate, nitric acid (5 mL) and deionized water (15 mL) to obtain the yellow homogeneous sol. Then the sol transformed into gel and dried at 105°C for 8 h to get xerogel. The obtained xerogel was crushed to 40–60 mesh, and calcined at 500°C with a heating rate of 10°C min^{-1} for 4 h in air. For comparison, MnO_x/TiO_2 (Mn/Ti) sample without Ce was synthesized by the same procedure. The catalysts were then characterized using powder X-ray diffraction analysis (XRD, XRD-6100; Shimadzu), N_2-physisorption with Brunauer-Emmet-Teller analysis (BET; ASAP-2020; Micromeritics), X-ray photoelectron spectroscope (XPS; ESCALAB 250; Thermo Fisher Scientific), hydrogen temperature-programmed reduction (H_2-TPR; Auto Chem II 2920) and ammonia temperature-programmed desorption (NH_3-TPD; Auto Chem II 2920). The notation and physicochemical properties of the catalysts are listed in Table 1.

Catalytic Activity Measurement

The NH_3-SCR of NO was carried out in a tubular quartz furnace (inner diameter × length = 20 mm × 500 mm) reactor, in which the catalyst powder was vertically loaded with the aid of a quartz screen. The catalyst was heated to the desired temperatures using an electric furnace under ambient pressure. NO (300 ppm), NH_3 (300 ppm), SO_2 (200 ppm when added), O_2 (0% and 3%) and N_2 (as balance) were fed to simulated flue gas. The total gas flow passing through 2 mL catalyst was controlled at 1000 mL min^{-1} by mass flow controllers, corresponding to a gas hourly space velocity (GHSV) of 30,000 h^{-1}. Each activity test operated after maintaining in steady condition for 1 h and repeated experiments were conducted to ensure the data reliability. The inlet concentration (C_{inlet}), outlet concentration (C_{outlet}) of NO were monitored by a flue gas analyzer (Optima 7.0; York Instruments Co., Ltd., Germany). The outlet concentration of NO_x ($C_{outlet\text{-}NOx}$) was concerned when focused on the NO_x yield from the over-oxidation of NH_3. NO conversion (%) and NO_x yield (%) are defined as:

$$\text{NO conversion (\%)} = (C_{inlet} - C_{outlet})/C_{inlet} \times 100\% \quad (1)$$

$$NO_x \text{ yield (\%)} = C_{outlet\text{-}NOx}/C_{inlet} \times 100\% \quad (2)$$

RESULTS AND DISCUSSION

Effect of Ce Doping on NH_3-SCR Activity of Mn/Ti Catalyst

A significant impact of Ce doping on Mn/Ti catalytic activity towards NH_3-SCR of NO is observed in Fig. 1. The highest NO conversion for $Mn_{0.15}$/Ti catalyst achieved at 200°C is merely 70%. Optimum condition occurs at $Mn_{0.15}Ce_{0.05}$/Ti catalyst, above 98% of NO can be abated even at 175°C. Further increase the Ce/Ti mole ratios to 0.1 or 0.15 reduces the catalytic activity of MnCe/Ti catalysts in the low-temperature range (< 200°C). Whereas, opposite trend is obtained above 200°C. For all the catalysts, NO conversion declines at high temperatures, while the turning point is postponed with the addition of Ce. Therefore, Ce addition not only improves the low-temperature catalytic performance of Mn/Ti catalysts but also broadens their active temperature window.

NH_3 oxidation with O_2 with or without the catalysts (Fig. 1) was implemented to ensure the assumption that the decline of NO conversion at high temperatures possibly attributes to the over-oxidation of the adsorbed NH_3 into NO_x. The NH_3 oxidation is barely observed in absence of catalyst and the presence of $Mn_{0.15}Ce_{0.05}$/Ti and $Mn_{0.15}Ce_{0.1}$/Ti catalysts

Table 1. The structure properties of Mn/Ti and MnCe/Ti catalysts.

Notation	Component molar ratio		S_{BET}[a] (m^2 g^{-1})	V_{micro}[a] (cm^3 g^{-1})	V_{tot}[a] (cm^3 g^{-1})	D[a] (nm)
	Mn/Ti	Ce/Ti				
$Mn_{0.15}$/Ti	0.15	/	78.6	0.023	0.146	7.4
$Mn_{0.15}Ce_{0.05}$/Ti	0.15	0.05	112.4	0.034	0.162	5.8
$Mn_{0.15}Ce_{0.10}$/Ti	0.15	0.10	115.3	0.036	0.176	4.7
$Mn_{0.15}Ce_{0.15}$/Ti	0.15	0.15	138.8	0.040	0.184	4.3

[a] Structure parameters of the catalysts got by N_2 adsorption-desorption; S_{BET}: BET surface area; V_{micro}: micropore volume; V_{tot}: total pore volume; D: average pore diameter.

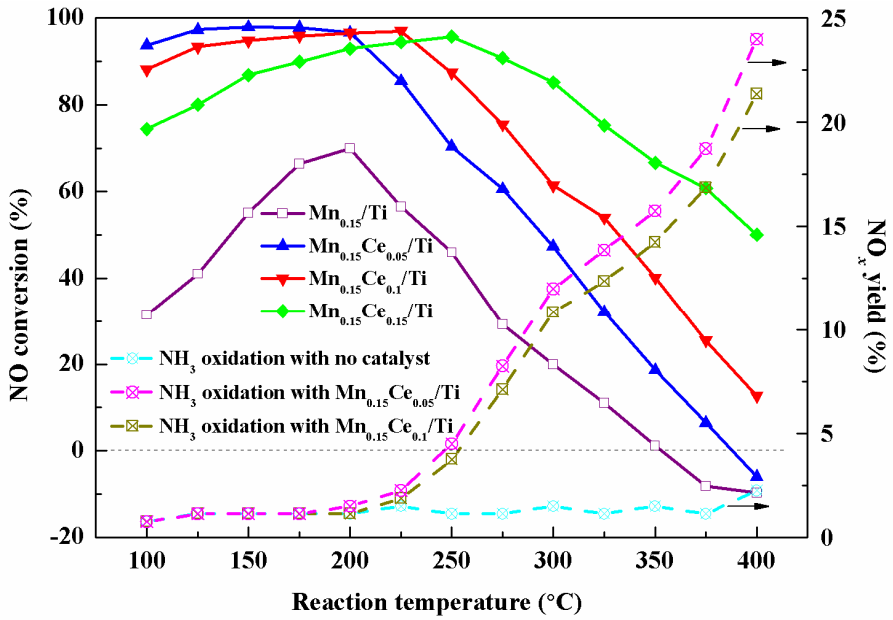

Fig. 1. NH_3-SCR activity of Mn/Ti and MnCe/Ti catalysts and NO_x yield with or without catalyst ($[NO]_{inlet}$ = $[NH_3]_{inlet}$ = 300 ppm, $[O_2]$ = 3%, N_2 as balance, GHSV = 30,000 h^{-1}).

facilitate the oxidation of NH_3 in the temperature range between 200–400°C. The higher NO_x yield from NH_3 oxidation on $Mn_{0.15}Ce_{0.05}$/Ti catalyst coincides with its lower catalytic activity at high temperatures, confirming the over-oxidation of the adsorbed NH_3 is the main reason for the reducing NO conversions at the temperature above 200°C.

Effect of Ce Doping on Catalyst Characterizations

XRD and BET Analysis

Several catalyst characterizations were conducted to gain insight into the multiple influences of the Ce addition on the structures and properties of the catalysts. The XRD patterns of Mn/Ti and MnCe/Ti catalysts are shown in Fig. 2. The diffraction peaks corresponding to anatase rather than rutile TiO_2 appear in all the tested catalysts. The MnO_2 at 37.2° (PDF#31-0820) and Mn_2O_3 at 55.2° (PDF#41-1422) are observed in $Mn_{0.15}$/Ti catalysts (Tang *et al.*, 2018). No obvious reflections assigned to the fluorite structure of CeO_2 can be observed for MnCe/Ti catalysts, except for a small peak at around 33.3°, which is attributed to (200) lattice plane of CeO_2 (Mao *et al.*, 2015; Deng *et al.*, 2016). Other reflections of CeO_2 are likely to be overlapped by the diffraction peaks of anatase TiO_2. In addition, MnCe/Ti catalysts also involve Ce_2O_3 showing a small diffraction peak at 30.2° (PDF#23-1048). The diffraction peaks belonging to Ce_2O_3 and CeO_2 become more intense and shift to higher Bragg angle when Ce/Ti mole ratio increases. The former occurs because the formed CeO_2 microcrystals grow and then cluster on TiO_2 surface with the increase of Ce/Ti mole ratio. The latter implies that the surrounding of Ce atom has been changed in combination with Mn atom. That is because the Mn atom radius (1.32 Å) is smaller than that of Ce (1.82 Å). The Mn atoms can be embedded in CeO_2 lattice surface (when Ce/Ti mole ratio = 0.05) or enter into CeO_2 lattice to replace some of the locations originally belonging to Ce atoms to form $MnCeO_x$ solid solution (when Ce/Ti mole ratio = 0.1, 0.15). These interactions between Mn and Ce atoms cause the shrinkage and distortion of CeO_2 lattice and result in such shifts of Ce_2O_3 and CeO_2 diffraction peaks in MnCe/Ti catalysts. Meanwhile, the signals corresponding to Mn species disappear when Ce is added. It is reasonable to believe that the phase structure of MnO_x is changed to amorphous phase after doping Ce, due either to the high dispersion of Mn species on catalyst support, or to the incorporation of partial Mn atoms to the fluorite structure of CeO_2 (Dai *et al.*, 2012). Both the above effects of Ce addition may be conducive to improve the catalytic activity of MnCe/Ti catalysts for NH_3-SCR of NO at low temperature.

As known, the SCR reaction is normally initiated with the adsorption of NH_3 (Kijlstra *et al.*, 1997), hence the adsorption capability of the catalysts is significantly important for NO abatement. It can be noticed in Table 1 that the S_{BET}, V_{tot} and V_{micro} values rise with the increase of Ce/Ti mole ratios and the D values are reduced accordingly. Literatures (Mastral *et al.*, 2000; Murillo *et al.*, 2004) have put forward that the gaseous reactant physisorption takes place mainly in the pores with the diameter close to the molecular size of the gaseous reactant, so that the adsorption potential is higher due to the proximity of the pore walls. Therefore, larger surface area, smaller average pore diameter and more abundant micropores (closer to the molecule sizes of NH_3 and NO which are smaller than 0.5 nm) contribute to the higher physisorption ability of MnCe/Ti catalysts. However, the $Mn_{0.15}Ce_{0.15}$/Ti catalyst with the highest physisorption ability exhibits the lowest catalytic activity at low temperature instead, implying that the physically adsorbed NH_3 might not be the main active species for further NO reduction. The chemisorption of NH_3 by surface acid sites forming activated transient state is probably available in SCR reaction (Ramis *et al.*, 1995).

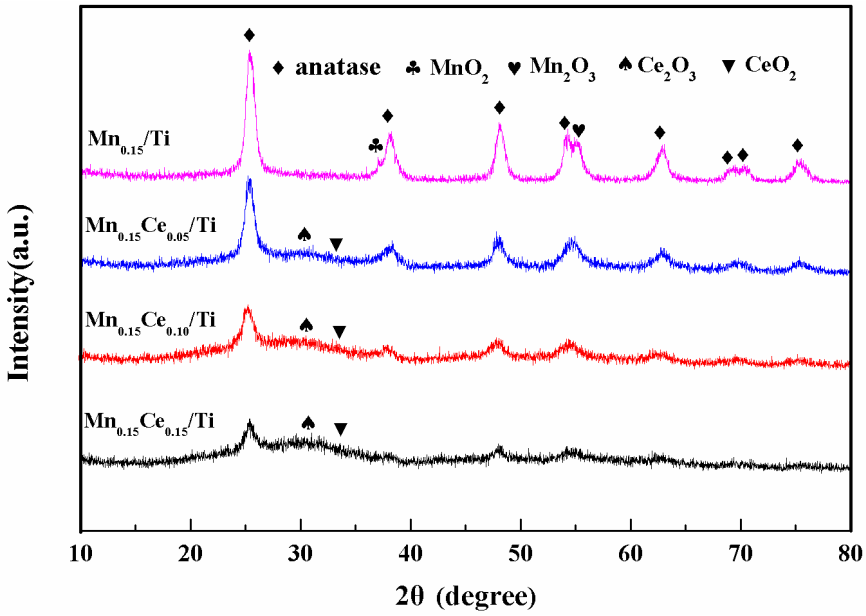

Fig. 2. XRD spectra of Mn/Ti and MnCe/Ti catalysts.

NH_3-TPD and H_2-TPR Analysis

NH_3-TPD experiments were carried out to evaluate the surface acid property (i.e., the amount and the strength) of the catalyst (Fig. 3(a)), which influences the chemisorption and activation of NH_3 (Li *et al.*, 2014). There are two NH_3 desorption peaks exists in the NH_3-TPD profile of all catalysts at 50–500°C. The NH_3 species anchored on Brønsted acidic sites are less thermally stable than the ones bonded to Lewis acidic sites (Li *et al.*, 2014; Nam *et al.*, 2017). Hence, the peaks at around 125°C and 300°C refer to the desorptions of the NH_3 adsorbed on weak Brønsted acid sites and strong Lewis acid sites (Chmielarz *et al.*, 2003), respectively. Many scholars held the opinion that the ammonium coordinated to Lewis acid sites (NH_3) are effective for NO reduction (Peña *et al.*, 2004; Wu *et al.*, 2007); ammonium ions adsorbed on Brønsted acid sites (NH_4^+) act as the 'reservoir' of the actively coordinated NH_3 species (i.e., $NH_{3(g)} + H^+ = NH_4^+{}_{(ads)} = NH_{3(ads)} + H^+$) and influence the SCR reaction indirectly (Qiu *et al.*, 2015). As seen from Fig. 3(a), the amounts of both Brønsted acid sites and Lewis acid sites of Mn/Ti catalyst are increased with the introduction of Ce. Besides, Ce addition enhances the strength of the Lewis acid sites on MnCe/Ti catalyst surface, for all the desorption peaks of the strongly adsorbed NH_3 species are shifted to higher temperature. The amount and strength of surface acid sites decrease following the order $Mn_{0.15}Ce_{0.05}$/Ti > $Mn_{0.15}Ce_{0.1}$/Ti > $Mn_{0.15}Ce_{0.15}$/Ti > $Mn_{0.15}$/Ti, which exactly matches their catalytic activities' variation tendency below 200°C, confirming that the surface acid property of the catalyst is one of the decisive factors for low-temperature NH_3-SCR activity.

Three reduction peaks on the TPR profile of $Mn_{0.15}$/Ti catalyst are observed in Fig. 3(b). The first two peaks at relatively low temperatures correspond to the reduction from MnO_2 or Mn_2O_3 to Mn_3O_4 and the last one centered at around 600°C refers to the further reduction from Mn_3O_4 to MnO (Liang *et al.*, 2008; Andreoli *et al.*, 2015). With the addition of Ce, the reduction peaks of MnCe/Ti catalysts become larger and start at lower-temperature regions. The former indicates the oxygen storage capacities of the catalysts are enlarged and the latter manifests the oxygen atoms in MnCe/Ti catalysts are easier to be offered to react with H_2. According to the starting position of the first reduction peak, the redox ability of the catalysts decreases in the order of $Mn_{0.15}Ce_{0.05}$/Ti > $Mn_{0.15}Ce_{0.1}$/Ti > $Mn_{0.15}Ce_{0.15}$/Ti > $Mn_{0.15}$/Ti, which agrees well with their NO conversions below 200°C. $Mn_{0.15}Ce_{0.05}$/Ti catalyst has excellent redox ability because the Mn atoms are more likely to be embedded in the CeO_2 microcrystal surface and hence highly dispersed. As the Ce/Ti mole ratios increase, the scattered reduction peaks tend to merge into one peak as shown in Fig. 3(b), implying the incorporation of Mn atoms into the CeO_2 lattice. The relatively low redox ability of the $Mn_{0.15}Ce_{0.1}$/Ti and $Mn_{0.15}Ce_{0.15}$/Ti catalysts is possibly due to the incorporation of Mn atoms into the bulk CeO_2 that reduces the surface exposed Mn atoms in consequence.

It is noteworthy that an opposite relationship between the redox ability of catalyst and the NO conversion at high-temperature region (> 200°C) is observed (Fig. 1). It possibly attributes to the excessively high redox ability of the catalysts causes the over-oxidation of the adsorbed NH_3 into NO_x. Inspired from the above results, catalyst with proper redox ability is preferred particularly at high temperatures so that over-oxidation of NH_3 can be alleviated or even avoided.

XPS Analysis

XPS was employed to investigate the surface element concentrations and oxidation states of the catalysts. High-resolution spectra from Mn 2p, Ce 3d, and O 1s are displayed in Fig. 4. The Mn 2p spectrum (Fig. 4(a)) suggests Mn species exist in a mixture of oxidation states on all the tested catalysts. According to the fitting results of XPS spectra, the Mn $2p_{2/3}$ signal can be deconvoluted into three characteristic

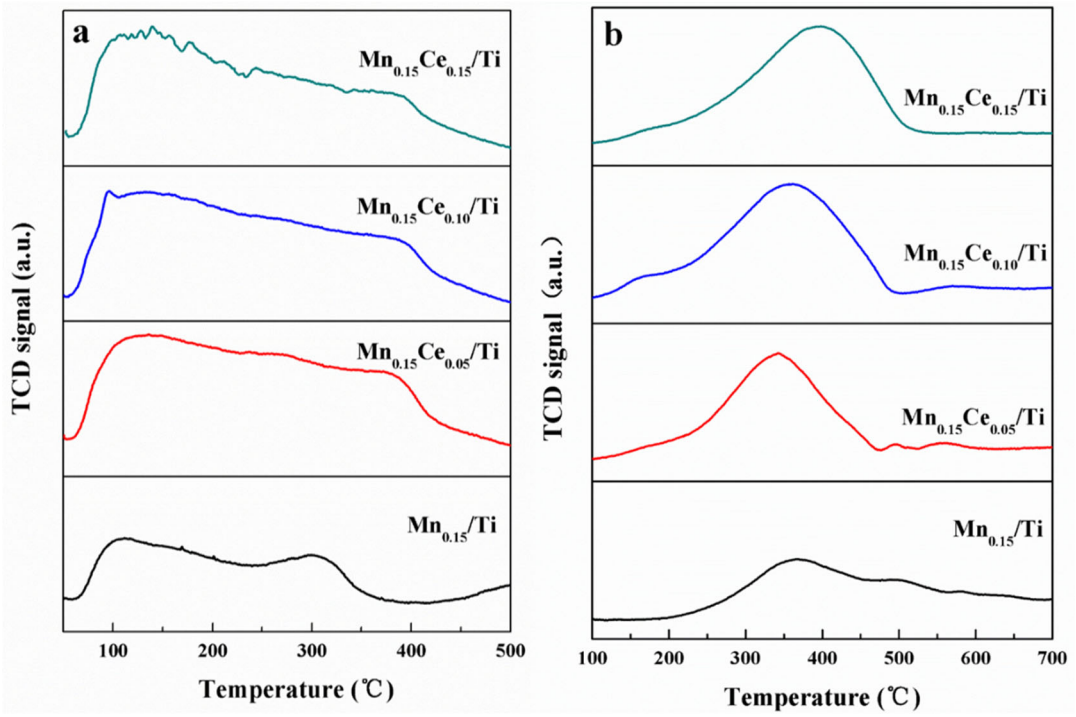

Fig. 3. (a) NH_3-TPD spectra and (b) H_2-TPR spectra of Mn/Ti and MnCe/Ti catalysts.

peaks, assigned to Mn^{4+} (643.4 eV), Mn^{3+} (641.9 eV) and Mn^{2+} (640.7 eV) respectively (Yu *et al.*, 2014). The Mn $2p_{1/2}$ signal also shows corresponding peaks from the above three Mn species in the bonding energy range 650–660 eV. As for the Ce 3d spectrum (Fig. 4(b)), all samples exhibit eight characteristic peaks in the range of 870–930 eV. The u′ and v′ peaks can be assigned to Ce^{3+} species, while the u‴, u″, u^0, v‴, v″, and v^0 peaks belong to Ce^{4+} species. Table 2 illustrates that the $Mn_{0.15}Ce_{0.05}$/Ti catalyst with the best catalytic performance has the most relative contents of surface Mn^{4+} and Ce^{3+} ions. It can be attributed to the addition of a small amount of Ce (Ce/Ti = 0.05) that prevents Mn atoms from entering into the bulk TiO_2 and leads to the high dispersion of Mn atom on catalyst surface (Dai *et al.*, 2011; Yao *et al.*, 2017). The highly dispersed surface Mn atoms are more likely to be oxidized to high-valence state (+4). Meanwhile, the electron transformation between Ce atom and the exposed Mn atom shifts the equilibrium "Mn^{3+} + Ce^{4+}↔Mn^{4+} + Ce^{3+}" (Ding *et al.*, 1998; Qi *et al.*, 2004; Xiong *et al.*, 2015) to the right and increases the Mn^{4+} and Ce^{3+} ions on catalyst surface. The former introduces more surface reactive oxygen species and has favorable redox properties for NO conversion (Yu *et al.*, 2014; Tang *et al.*, 2015); the latter has been used as an indicator for the surface defect structures (e.g., oxygen vacancies) in ceria-based materials (Tang *et al.*, 2015). Oxygen vacancies driven by redox cycle between Ce^{4+} and Ce^{3+} promote the migration of the oxygen species, which is beneficial to the oxidation of NO to NO_2 and further enhances NO conversion through 'fast NH_3-SCR' (Xiong *et al.*, 2015). Unexpectedly, the surface Mn^{4+} and Ce^{3+} ions are conversely reduced when further increase the Ce/Ti mole ratios. That is because the crystalline structure of excessive CeO_2 preferentially take the Mn atom into its bulk phase and reduce the exposed Mn atom on catalyst surface. In this case, we speculate the above redox equilibrium probably shifts to the left, which results in the abatement of Mn^{4+} and Ce^{3+} ions on the surface of $Mn_{0.15}Ce_{0.1}$/Ti and $Mn_{0.15}Ce_{0.15}$/Ti catalysts. These are the important reasons that explains their poorer SCR activity at low temperatures.

As shown in Fig. 4(c), the O1s XPS spectra of all catalysts present two main peaks belonging to the surface chemisorbed oxygen (labeled as O_α) and surface lattice oxygen (labeled as O_β) (Li *et al.*, 2011; Meng *et al.*, 2015). Hereinto, the O_α referred to the oxygen free radicals (e.g., O, O^- and O_2^-) are weakly bonded to surface metal atoms and easier to be offered in oxidation-reduction reaction. Therefore, the highest concentration ratio of $O_\alpha/(O_\alpha + O_\beta)$ in $Mn_{0.15}Ce_{0.05}$/Ti catalyst contributes to its best low-temperature catalytic activity towards NO conversion. Besides, O_β peak is also observed shifting to higher binding energy in $Mn_{0.15}Ce_{0.05}$/Ti catalyst, suggesting that adding a small amount of Ce also weakens the interaction between metal atoms and O_β, and makes the O_β easier to be offered to oxidize reactants. Further increase the Ce/Ti mole ratios raises the total surface oxygen atomic contents from 74.7% ($Mn_{0.15}Ce_{0.05}$/Ti) to 76.3% ($Mn_{0.15}Ce_{0.1}$/Ti) and 76.4% ($Mn_{0.15}Ce_{0.15}$/Ti), but the $O_\alpha/(O_\alpha + O_\beta)$ values as well as the O_β binding energies of $Mn_{0.15}Ce_{0.1}$/Ti and $Mn_{0.15}Ce_{0.15}$/Ti catalysts are dropped instead. This phenomenon indicates that Ce addition enlarges the oxygen storage capacity of the catalyst, while the mobility of the oxygen atom relates with the exposure of Mn atom. It agrees well with the result of ref. (Lee *et al.*, 2012), the authors believed that such an exposed Mn atom shows a direct correlation with the activity of MnCe/Ti catalyst.

The above assumption that Ce addition amount influences the exposure of Mn atom can be further evidenced by

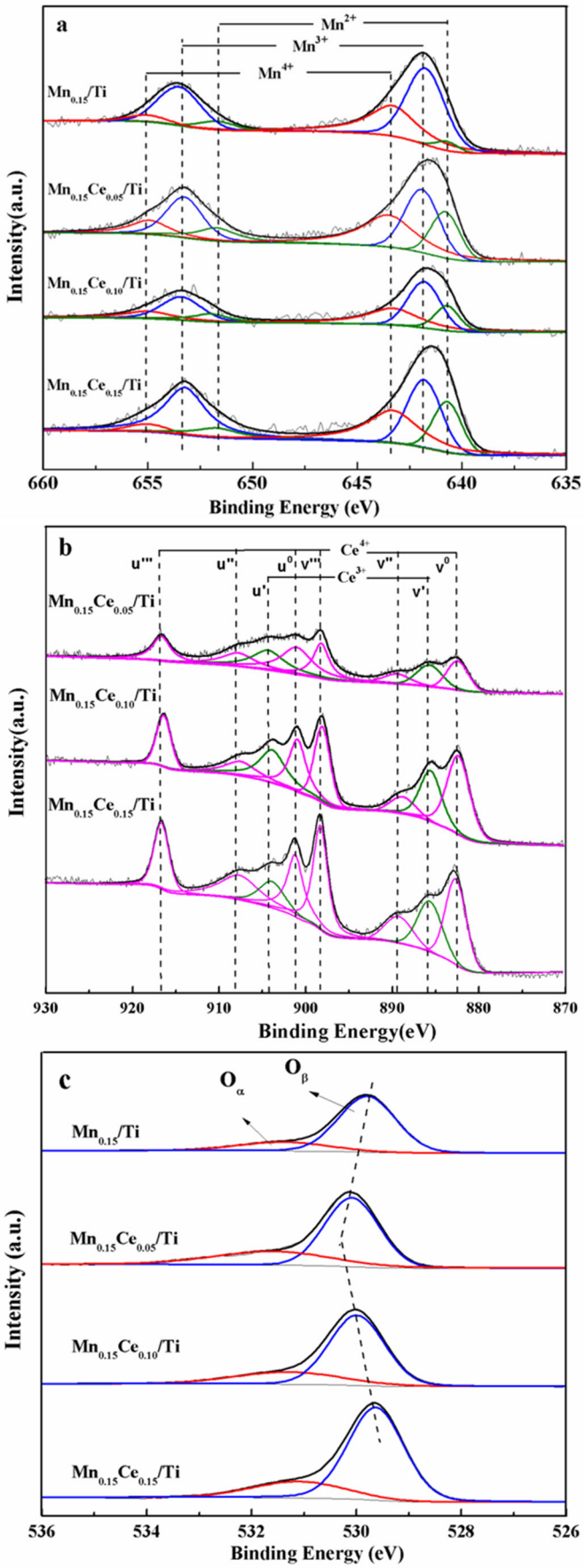

Fig. 4. (a) Mn 2p, (b) Ce 3d and (c) O 1s XPS spectra of the Mn/Ti and MnCe/Ti catalysts.

Table 2. The surface atomic concentration and valence state distribution of Mn/Ti and MnCe/Ti catalysts.

Samples	Mn (at %)[a]	Mn valence state distribution			Ce (at %)[a]	Ce valence state distribution		O (at %)[a]	$O_\alpha/(O_\alpha + O_\beta)$	Ti (at %)[a]	Mn/(Ce + Ti)[b]	Ce/(Mn + Ti)[b]
		Mn^{4+} (%)	Mn^{3+} (%)	Mn^{2+} (%)		Ce^{4+} (%)	Ce^{3+} (%)					
$Mn_{0.15}/Ti$	3.3	25.5	48.5	26.0	/	/	/	71.4	0.20	25.3	0.13 (0.15)[c]	/
$Mn_{0.15}Ce_{0.05}/Ti$	3.7	35.7	41.7	22.5	0.8	71.3	28.7	74.7	0.28	20.8	0.17 (0.14)	0.03 (0.04)[c]
$Mn_{0.15}Ce_{0.10}/Ti$	1.8	33.2	46.8	19.9	1.3	72.0	28.0	76.3	0.25	20.6	0.08 (0.14)	0.06 (0.09)
$Mn_{0.15}Ce_{0.15}/Ti$	1.6	29.7	48.1	22.2	1.5	74.3	25.7	76.4	0.22	20.5	0.07 (0.13)	0.07 (0.13)

[a] The surface element compositions of Mn, Ce and O estimated by XPS analysis.
[b] The actual Mn/(Ce + Ti) and Ce/(Mn + Ti) mole ratios obtained from the XPS results.
[c] The theoretical Mn/(Ce + Ti) and Ce/(Mn + Ti) mole ratios calculated according to the preparation processes.

comparing the actual Mn/(Ce + Ti) and Ce/(Mn + Ti) mole ratios with their theoretical values (Table 2). Accordingly, an assumption model is proposed in Fig. 5. As for $Mn_{0.15}/Ti$ catalyst, the actual Mn/(Ce + Ti) mole ratio (0.13) is slightly lower than the theoretical value (0.15) due either to the Mn atoms entering the bulk TiO_2 or the presence of MnO_x crystals (in line with the XRD patterns) resulting in the poor distribution of the Mn atoms (Fig. 5(a)). After adding a small amount of Ce (Ce/Ti = 0.05), the actual Ce/(Mn + Ti) value of $Mn_{0.15}Ce_{0.05}/Ti$ catalyst (0.03) is close to the theoretical mole ratio (0.04); the actual Mn/(Ce + Ti) mole ratio of $Mn_{0.15}Ce_{0.05}/Ti$ catalyst (0.17) become clearly larger than its theoretical value (0.14). It indicates that more Mn atoms are exposed and better dispersed on catalyst surface (in agreement with XRD patterns), because the highly dispersed CeO_2 microcrystal prevents the Mn atoms from entering into the bulk TiO_2 (Fig. 5(b)). As for $Mn_{0.15}Ce_{0.1}/Ti$ and $Mn_{0.15}Ce_{0.15}/Ti$, their actual Ce/(Mn + Ti) values (0.06 and 0.07) are greatly lower than their theoretical values (0.09 and 0.13). Considering the radius of Ce atom (1.82 Å) is larger than that of Ti (1.45 Å), it is difficult for Ce atom getting into TiO_2 lattice. So, it is reasonable to believe that the lower actual Ce/(Mn + Ti) values of $Mn_{0.15}Ce_{0.1}/Ti$ and $Mn_{0.15}Ce_{0.15}/Ti$ catalysts result from the agglomeration of CeO_2 crystals (in line with XRD patterns) on TiO_2 surface which causes the poor dispersion of CeO_2. Coincidentally, both the actual Mn/(Ce + Ti) mole ratio values of $Mn_{0.15}Ce_{0.1}/Ti$ (0.08) and $Mn_{0.15}Ce_{0.15}/Ti$ (0.07) are obviously lower than their theoretical values (0.14 and 0.13). It coincides with the conjecture that the exposed surface Mn atoms are significantly decreased due to the incorporation of Mn atom into the bulk of CeO_2 crystal which agglomerates on the TiO_2 surface as shown in Fig. 5(c).

NH_3-SCR in Oxygen-rich and Oxygen-free Atmosphere

NH_3-SCR of NO under oxidizing/reducing conditions were carried out to investigate the oxygen storage/release capability of the Mn/Ti and MnCe/Ti catalysts. The experimental result shown in Fig. 6 demonstrates that NH_3-SCR reaction still takes place in oxygen-free atmosphere and indicates that the reactive oxygen species in catalyst participates in NH_3-SCR of NO. Ce addition can alleviate the deactivation of the catalysts in oxygen-free atmosphere effectively and the NO conversion of $Mn_{0.15}Ce_{0.05}/Ti$ catalyst in oxygen-free atmosphere maintains at around 80% at 200°C for even 10 hours as shown in the inset of Fig. 6. The less deactivation in $Mn_{0.15}Ce_{0.05}/Ti$ catalyst probably because there are abundant exposed Mn^{4+} ions on $Mn_{0.15}Ce_{0.05}/Ti$ catalyst surface can activate the adsorbed $NH_{3(ads)}$ (Reactions (3)–(4)); meanwhile release sufficient reactive oxygen species for $NO_{(ads)}$ oxidation (Reaction (5)) in oxygen-free atmosphere. However, the reoxidation of the reduced Mn atom (Reaction (6)) is blocked in oxygen-free atmosphere and thus results in the deactivation of catalysts.

$$Mn^{4+} + NH_{3(ads)} \rightarrow Mn^{3+} + –NH_2 + H^+ \quad (3)$$

$$Mn^{4+} + –NH_2 \rightarrow Mn^{3+} + –NH + H^+ \quad (4)$$

$$Mn^{4+} – O + NO_{(ads)} \rightarrow Mn^{3+} + NO_{2(ads)} \quad (5)$$

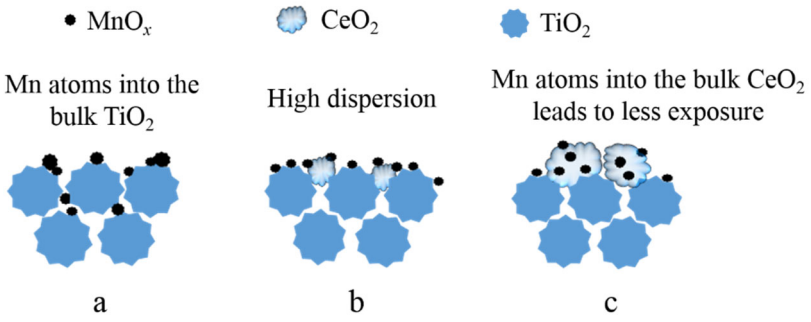

Fig. 5. An assumption model for (a) Mn/Ti and (b–c) MnCe/Ti catalysts.

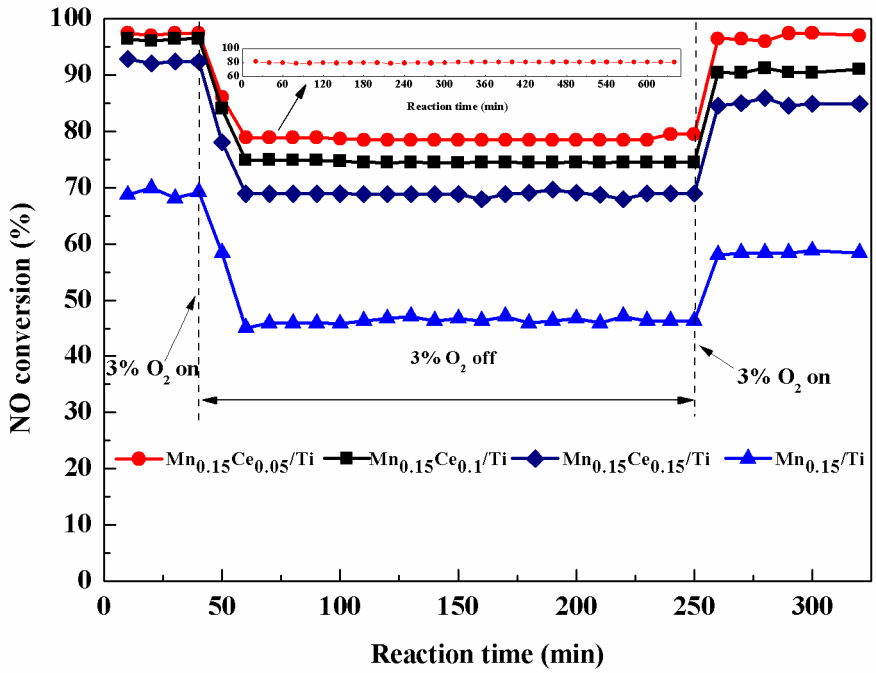

Fig. 6. NH_3-SCR activities of Mn/Ti and MnCe/Ti catalysts with or without O_2 ($[NO]_{inlet} = [NH_3]_{inlet}$ = 300 ppm, $[O_2]$ = 3%, N_2 as balance, GHSV = 30,000 h^{-1}, temperature = 200°C).

$$Mn^{3+} + 1/2O_2 \rightarrow Mn^{4+} - O \quad (6)$$

$$Mn^{3+} + NO_{2(g)} \rightarrow Mn^{4+} + -NO_2^- \quad (7)$$

As soon as O_2 is reinjected into the reaction atmosphere, the NO conversions rise again in all catalysts within 10 min. That is because the oxygen vacancies can be replenished with O_2 by reoxidizing the Mn atoms from +3 to +4 (Reaction (6)). In addition, the $NO_{2(g)}$ generated from the oxidation of NO with O_2 also help reoxidize the reduced metal atom (Reaction (7)). As seen from Fig. 6, the deactivated $Mn_{0.15}Ce_{0.05}$/Ti catalyst can be completely regenerated at 200°C, while the deactivation in other catalysts seems to be irreversible under this condition. That is because the exposed Mn atoms embedded in the surface of CeO_2 microcrystal contributes to a flexible redox cycle between Mn^{4+} and Mn^{3+}. This phenomenon supports the result that the oxygen release/storage capability of $Mn_{0.15}Ce_{0.05}$/Ti catalyst is higher than those of the other two catalysts, which is another determining factor for its high NH_3-SCR activity at low temperatures.

NH_3-SCR in SO_2-containing Atmosphere

Temperature-dependent effect of SO_2 on NH_3-SCR of NO over $Mn_{0.15}Ce_{0.05}$/Ti catalyst is obtained in Fig. 7(a). As observed, SO_2 suppresses the SCR performance at 100–275°C. Nevertheless, still more than 75% NO conversion is provided by $Mn_{0.15}Ce_{0.05}$/Ti catalyst after SO_2 poisoning at 175°C and that is even higher than the optimum value of $Mn_{0.15}$/Ti catalyst obtained in SO_2-free atmosphere. This result implies that Ce modification can enhance the SO_2 resistance of MnCe/Ti catalyst at low temperature, which coincides with the observations reported in previous studies (Zhu *et al.*, 2001; Wang *et al.*, 2015; Li *et al.*, 2016). The improvement of Ce addition on SO_2 resistance of Ce-modified Mn/Ti catalyst attributes to two main reasons. Firstly, Ce doping inhibits the depositions of ammonia sulfites and sulfates that would block the active sites and affect the oxidation properties of the catalyst (Wu *et al.*, 2009; Jin *et al.*, 2014; Wang *et al.*, 2015). Secondly, surface sulfates are preferentially

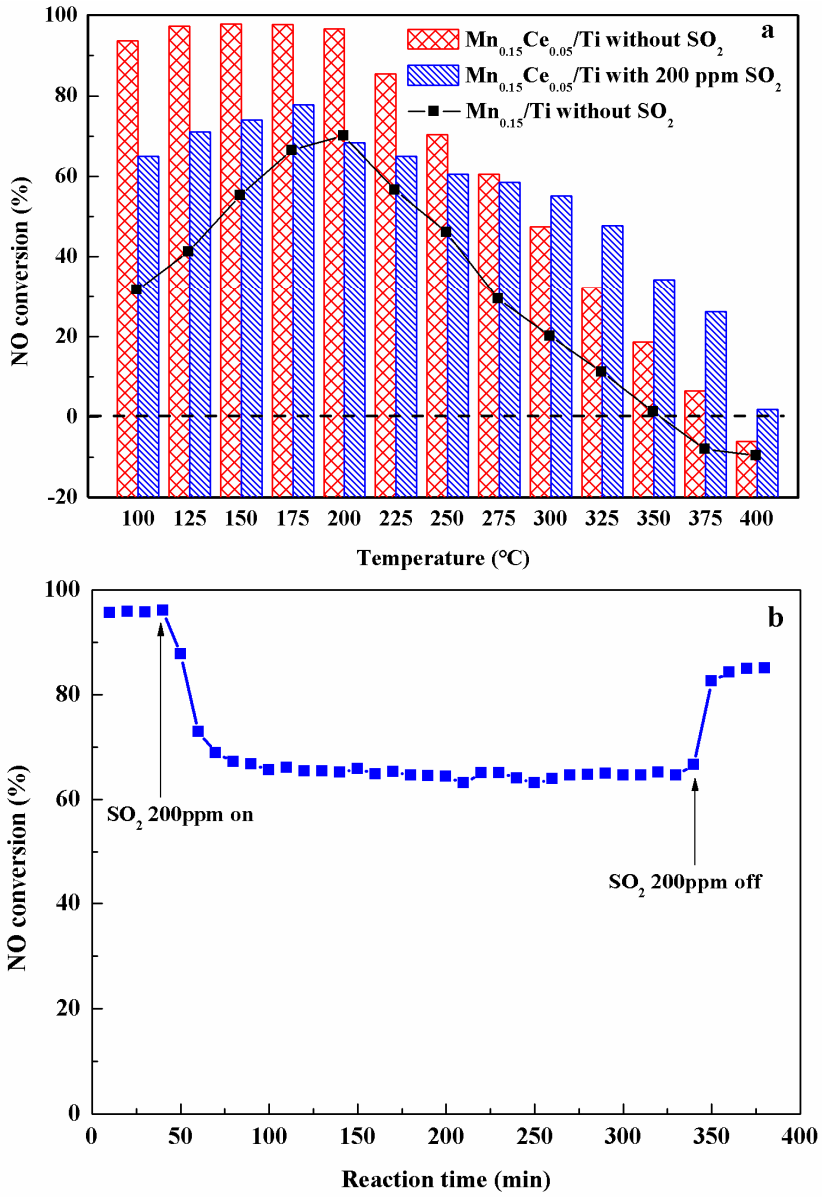

Fig. 7. (a) Effect of SO_2 on NH_3-SCR activity and (b) transient response of SO_2 on $Mn_{0.15}Ce_{0.05}$/Ti catalyst ($[NO]_{inlet}$ = $[NH_3]_{inlet}$ = 300 ppm, $[O_2]$ = 3%, SO_2 = 200 ppm (when added), N_2 as balance, GHSV = 30,000 h^{-1}, temperature = 200°C).

formed on Ce dopants in presence of SO_2, which lessens the sulfation of the main active phase (MnO_x) (Jin *et al.*, 2014; Ma *et al.*, 2019). On the contrary, SO_2 presents a positive effect on NH_3-SCR reaction over $Mn_{0.15}Ce_{0.05}$/Ti catalyst above 300°C, which is in good agreement with Ma *et al.* (2013)'s observations. That is because the depositions of ammonia sulfites and sulfates are reduced and the formation of metal sulfates (e.g., $Ce_2(SO_3)_3$ or $Ce(SO_4)_2$) is facilitated at high temperatures (Ma *et al.*, 2013; Wang *et al.*, 2015). The latter reduces the oxidation ability of $Mn_{0.15}Ce_{0.05}$/Ti catalyst and thereby minimizes the over-oxidation of NH_3, which is the main side reaction (in Section 3.1) responsible for the reduction of SCR activity at high temperatures (Xie *et al.*, 2004).

The transient response of SO_2 poisoning was also carried out on $Mn_{0.15}Ce_{0.05}$/Ti catalyst at 200°C and the result is shown in Fig. 7(b). The NO conversion declines from 96% to 65% within 20 min and then remains stable for 300 min after introducing 200 ppm SO_2. As mentioned above, the sulfation is preferentially happened on Ce dopants which disrupts the Ce^{4+}/Ce^{3+} redox cycle. As such, more sulfates have been stored in ceria; less ammonia sulfites and sulfates could be further formed to cover the catalyst surface (Jin *et al.*, 2014). Besides, Jin *et al.* (2014) proposed that Ce doping could reduce the thermal stability of the ammonia sulfites and sulfates on MnCe/Ti catalyst based on their theoretical calculation. For this reason, the deposition and decomposition of ammonia sulfites and sulfates on catalyst surface can easily reach a balance and hence the long-term stable SCR activity of $Mn_{0.15}Ce_{0.05}$/Ti can be achieved in presence of SO_2. As soon as SO_2 is removed off, NO conversion can be restored to 82% but is still slightly lower than the original

one. The SCR activity can be mostly recovered after shutting SO_2 off, because the ammonia sulfites and sulfates can be easily removed from the $Mn_{0.15}Ce_{0.05}$/Ti surface. However, the deactivation caused by the sulfation of Ce dopants is irreversible under this condition that explains the difference between the restored and the original SCR performance. Therefore, thermal treatment at higher temperature (> 350°C) is suggested for it has the possibility to fully recover the catalyst activity after SO_2 poisoning (Wang *et al.*, 2015).

CONCLUSION

Incorporating Ce significantly enhances the activity of Mn/Ti catalysts, with the maximum effect being exhibited by catalysts possessing Mn/Ti and Ce/Ti ratios of 0.15 and 0.05, respectively. The catalytic activity of the MnCe/Ti catalyst is directly correlated with the number of exposed Mn atoms, which increases with the addition of a small amount of Ce (Ce/Ti = 0.05), thus improving the oxygen storage/release capability of the catalyst. However, the presence of excessive CeO_2 reduces the exposure of the surface Mn due to the incorporation of the latter into the bulk CeO_2, thereby decreasing the catalytic activity of the $Mn_{0.15}Ce_{0.1}$/Ti and $Mn_{0.15}Ce_{0.15}$/Ti catalysts at low temperatures. The addition of Ce can also increase the SO_2 resistance of Mn/Ti catalysts by (1) inhibiting the deposition of ammonia sulfites and sulfates on the catalyst surface and (2) reducing the sulfation of the main active phase (MnO_x). Furthermore, SO_2 facilitates the SCR of $Mn_{0.15}Ce_{0.05}$/Ti catalysts above 300°C because more surface sulfates are preferentially formed on the Ce dopant, which suppresses the over-oxidation of NH_3 at high temperatures by reducing the oxidation ability of the catalyst.

ACKNOWLEDGEMENTS

This research is supported by Natural Science Foundation of Shanghai (17ZR1419400), National Key R&D Program of China (2018YFC1901204), National Natural Science Foundation of China (51706156 and 51976129) and Shanghai Rising-Star Program (17QC1401000).

REFERENCES

Andreoli, S., Deorsola, F.A. and Pirone, R. (2015). MnO_x-CeO_2 catalysts synthesized by solution combustion synthesis for the low-temperature NH_3-SCR. *Catal. Today* 253: 199–206.

Chang, H.Z., Chen, X.Y., Li, J.H. and Ma, L. (2013). Improvement of activity and SO_2 tolerance of Sn-modified MnO_x-CeO_2 catalysts for NH_3-SCR at low temperatures. *Environ. Sci. Technol.* 47: 5294–5301.

Chmielarz, L., Kuśtrowski, P., Zbroja, M., Łasocha, A.R., Dudek, B. and Dziembaj, R. (2003). SCR of NO by NH_3 on alumina or titania-pillared montmorillonite various modified with Cu or Co: Part I. General characterization and catalysts screening. *Appl. Catal., B* 45: 103–116.

Dai, Y., Wang, X.Y., Li, D. and Dai, Q.G. (2011). Catalytic combustion of chlorobenzene over Mn-Ce-La-O mixed oxide catalysts. *J. Hazard. Mater.* 188: 132–139.

Dai, Y., Wang, X.Y., Dai, Q.G. and Li, D. (2012). Effect of Ce and La on the structure and activity of MnO_x catalyst in catalytic combustion of chlorobenzene. *Appl. Catal., B* 111–112: 141–149.

Deng, W., Dai, Q.G., Lao, Y.J., Shi, B.B. and Wang, X.Y. (2016). Low temperature catalytic combustion of 1,2-dichlorobenzene over CeO_2–TiO_2 mixed oxide catalysts. *Appl. Catal., B* 181: 848–861.

Ding, Z.Y., Li, L.X., Daniel, W. and Earnest F.G. (1998). Supercritical water oxidation of NH_3 over a MnO_2/CeO_2 Catalyst. *Ind. Eng. Chem. Res.* 37: 1707–1716.

Ettireddy, P.R., Ettireddy, N., Mamedov, S., Boolchand, P. and Smirniotis, P.G. (2007). Surface characterization studies of TiO_2 supported manganese oxide catalysts for low temperature SCR of NO with NH_3. *Appl. Catal., B* 76: 123–134.

Fan, Y.M., Ling, W., Dong, L.F., Li, S.H., Yu, C.L., Huang, B.C. and Xi, H.X. (2018). *In situ* FT-IR and DFT study of the synergistic effects of cerium presence in the framework and the surface in NH_3-SCR. *Aerosol Air Qual. Res.* 18: 655–670.

Jiang, Y., Wang, X.C., Xing, Z.M., Bao, C.Z. and Liang, G.T. (2017). Preparation and characterization of CeO_2-MoO_3/TiO_2 catalysts for selective catalytic reduction of NO with NH_3. *Aerosol Air Qual. Res.* 17: 2726–2734.

Jiang, Y., Bao, C.Z., Liu, S.J., Liang, G.T., Lu, M.Y. Lai, C.Z., Shi, W.Y. and Ma, S.Y. (2018). Enhanced activity of Nb-modified CeO_2/TiO_2 catalyst for the selective catalytic reduction of NO with NH_3. *Aerosol Air Qual. Res.* 18: 2121–2130.

Jin, R.B., Liu, Y., Wang, Yan., Cen, W.L., Wu, Z.B., Wang, H.Q. and Weng, X.L. (2014). The role of cerium in the improved SO_2 tolerance for NO reduction with NH_3 over Mn-Ce/TiO_2 catalyst at low temperature. *Appl. Catal., B* 148–149: 582–588.

Kijlstra, W.S., Brands, D.S., Smit, H.I., Poels, E.K. and Bliek, A. (1997). Mechanism of the selective catalytic reduction of NO with NH_3 over MnO_x/Al_2O_3. *J. Catal.* 171: 219–230.

Kwon, D.W., Nam, K.B. and Hong, S.C. (2015). The role of ceria on the activity and SO_2 resistance of catalysts for the selective catalytic reduction of NO_x by NH_3. *Appl. Catal., B* 166–167: 37–44.

Lee, S.M., Park, K.H. and Hong, S.C. (2012). MnO_x/CeO_2–TiO_2 mixed oxide catalysts for the selective catalytic reduction of NO with NH_3 at low temperature. *Chem. Eng. J.* 195–196: 323–331.

Li, B., Ren, Z.Y., Ma, Z.X., Huang, X.D., Liu, F., Zhang, X.B. and Yang, H.S. (2016). Selective catalytic reduction of NO by NH_3 over CuO-CeO_2 in the presence of SO_2. *Catal. Sci. Technol.* 6: 1719–1725.

Li, J.F., Yan, N.Q., Qu, Z., Qiao, S.H., Yang, S.J., Guo, Y.F., Liu, P. and Jia, J.P. (2014). Catalytic oxidation of elemental mercury over the modified catalyst Mn/alpha-Al_2O_3 at lower temperatures. *Environ. Sci. Technol.* 44: 426–431.

Li, Q., Yang, H.S., Qiu, F.M. and Zhang, X.B. (2011). Promotional effects of carbon nanotubes on V_2O_5/TiO_2

for NO_x removal. *J. Hazard. Mater.* 192: 915–921.

Liang, S.H., Teng, F., Bulgan, G. and Zong, R.L. (2008). Effect of phase structure of MnO_2 nanorod catalyst on the activity for CO oxidation. *J. Phys. Chem. C.* 112: 5307–5315.

Long, R.Q. and Yang, R.T. (2000). The promoting role of rare earth oxides on Fe-exchanged TiO_2-pillared clay for selective catalytic reduction of nitric oxide by ammonia. *Appl. Catal., B* 27: 87–95

Ma, Z.R., Wu, X.D., Si, Z.C., Weng, D., Ma, J. and Xu, T.F. (2015). Impacts of niobia loading on active sites and surface acidity in NbO_x/CeO_2-ZrO_2 NH_3-SCR catalysts. *Appl. Catal., B* 179: 380–394.

Ma, Z.X., Yang, H.S., Li, B., Liu, F. and Zhang, X.B. (2013). Temperature-Dependent effects of SO_2 on selective catalytic reduction of NO over Fe-Cu-O_x/CNTs-TiO_2 catalysts. *Ind. Eng. Chem. Res.* 52: 3708–3713.

Ma, Z.X., Sheng, L.P., Wang, X.W., Yuan, W.T., Chen, S.Y., Xue, W., Han, G.R., Zhang, Z., Yang, H.S., Lu, Y.H. and Wang, Y. (2019). Oxide catalysts with ultrastrong resistance to SO_2 deactivation for removing nitric oxide at low temperature. *Adv. Mater.* 31: 1903719.

Mao, D., He, F., Zhao, P. and Liu, S.T. (2015). Enhancement of resistance to chlorine poisoning of Sn-modified MnCeLa catalysts for chlorobenzene oxidation at low temperature. *RSC. Adv.* 5: 10040–10047.

Mastral, A.M., Garcia, T., Callen, M. and Navarro, M.V. (2000). Assessement of phenanthrene removal from hot gas by porous carbons. *Energy Fuels* 15: 1–7.

Meng, D.M., Zhan, W.C., Guo, Y. and Guo, Y.L. (2015). A highly effective catalyst of Sm-MnO_x for the NH_3-SCR of NO_x at low temperature: Promotional role of Sm and its catalytic performance. *ACS Catal.* 5: 5973–5983.

Murillo, R., García, T., Aylón, E., Callén, M.S., Navarro, M.V., López, J.M. and Mastral, A.M. (2004). Adsorption of phenanthrene on activated carbons: Breakthrough curve modeling. *Carbon* 42: 2009–2017.

Nam, K.B., Kwon, D.W. and Hong, S.C. (2017). DRIFT study on promotion effects of tungsten-modified Mn/Ce/Ti catalysts for the SCR reaction at low-temperature. *Appl. Catal., A* 542: 55–62.

Peña, D.A., Uphade, B.S., Reddy, E.P. and Smirniotis, P.G. (2004). Identification of surface species on titania-supported manganese, chromium, and copper oxide low-temperature SCR catalysts. *J. Phys. Chem. B* 108: 9927–9936.

Qi, G.S., Yang, R.T. and Chang, R. (2003). Low-temperature SCR of NO with NH_3 over USY-supported manganese oxide-based catalysts. *Catal. Lett.* 87: 67–71.

Qi, G.S., Yang, R.T. and Chang, R. (2004). MnO_x-CeO_2 mixed oxides prepared by co-precipitation for selective catalytic reduction of NO with NH_3 at low temperatures. *Appl. Catal., B* 51: 93–106.

Qiu, L., Pang, D.D., Zhang, C.L., Meng, J.J., Zhu, R.S. and Feng, O.Y. (2015). In situ IR studies of Co and Ce doped Mn/TiO_2 catalyst for low-temperature selective catalytic reduction of NO with NH_3. *Appl. Surf. Sci.* 357: 189–196.

Ramis, G., Yi, L., Busca, G., Turco, M., Kotur, E. and Willey, R.J. (1995). Adsorption, activation, and oxidation of ammonia over SCR catalysts. *J. Catal.* 157: 523–535.

Roy, S., Hegde, M.S. and Madras, G. (2009). Catalysis for NO_x abatement. *Appl. Energy* 86: 2283–2297.

Song, H., Zhang, M.L., Yu, J.P., Wu, W.H., Qu, R.Y., Zheng, C.H. and Gao, X. (2017). The effect of Cr addition on Hg^0 oxidation and NO reduction over V_2O_5/TiO_2 catalyst. *Aerosol Air Qual. Res.* 18: 803–810.

Sultana, A., Sasaki, M. and Hamada, H. (2012). Influence of support on the activity of Mn supported catalysts for SCR of NO with ammonia. *Catal. Today* 185: 284–289.

Tang, A., Hu, L.Q., Yang, X.H., Jia, Y.R. and Zhang, Y. (2018). Promoting effect of the addition of Ce and Fe on manganese oxide catalyst for 1,2-dichlorobenzene catalytic combustion. *Catal. Commun.* 82: 41–45.

Tang, C.J., Li, J.C., Yao, X.J., Sun, J.F., Cao, Y., Zhang, Lei., Gao, F., Deng, Y. and Dong, L. (2015). Mesoporous NiO-CeO_2 catalysts for CO oxidation: Nickel content effect and mechanism aspect. *Appl. Catal., A* 494: 77–86.

Tang, C.J., Zhang, H.L. and Dong, L. (2016). Ceria-based catalysts for low-temperature selective catalytic reduction of NO with NH_3. *Catal. Sci. Technol.* 5: 1248–1264.

Tang, X.L., Hao, J.M., Yi, H.H. and Li, J.H. (2007). Low-temperature SCR of NO with NH_3 over AC/C supported manganese-based monolithic catalysts. *Catal. Today* 126: 406–411.

Tian, W., Fan, X.Y., Yang, H.S. and Zhang, X.B. (2010). Preparation of MnO_x/TiO_2 composites and their properties for catalytic oxidation of chlorobenzene. *J. Hazard. Mater.* 177: 887–891.

Wang, L.S., Huang, B.C., Su, Y.X., Zhou, G.Y., Wang, K.L., Luo, H.C. and Ye, D.Q. (2012). Manganese oxides supported on multi-walled carbon nanotubes for selective catalytic reduction of NO with NH_3: Catalytic activity and characterization. *Chem. Eng. J.* 192: 232–241.

Wang, Y., Li, X., Zhan, L., Li, C., Qiao, W. and Ling, L. (2015). Effect of SO_2 on activated carbon honeycomb supported CeO_2-MnO_x catalyst for NO removal at low temperature. *Ind. Eng. Chem. Res*. 554: 2274–2278.

Wu, Z.B., Jiang, B.Q., Liu, Y., Wang, H.Q. and Jin, R.B. (2007). DRIFT study of manganese/titania-based catalysts for low-temperature selective catalytic reduction of NO with NH_3. *Environ. Sci. Technol.* 41: 5812–5817.

Wu, Z.B., Jin, R.B., Wang, H.Q. and Liu, Y. (2009). Effect of ceria doping on SO_2 resistance of Mn/TiO_2 for selective catalytic reduction of NO with NH_3 at low temperature. *Catal. Commun.* 10: 935–939.

Xie, G.Y., Liu, Z.Y., Zhu, Z.P., Liu, Q.Y., Ge, J. and Huang, Z.G. (2004). Simultaneous removal of SO_2 and NO_x from flue gas using a CuO/Al_2O_3 catalyst sorbent I. Deactivation of SCR activity by SO_2 at low temperatures. *J. Catal.* 224: 36–41.

Xiong, Y., Tang, C.J., Yao, X.J., Zhang, L., Li, L.L., Wang, X.B., Deng, Y., Gao, F. and Dong, L. (2015). Effect of metal ions doping (M = Ti^{4+}, Sn^{4+}) on the catalytic performance of MnO_x/CeO_2 catalyst for low temperature selective catalytic reduction of NO with NH_3. *Appl. Catal., A* 495: 206–216.

Yang, Y., Huang, J., Wang, S.W., Deng, S.B., Wang, B. and Yu, G. (2013). Catalytic removal of gaseous unintentional

POPs on manganese oxide octahedral molecular sieves. *Appl. Catal., B* 142–143: 568–578.

Yao, X.J., Kaili, M., Zou, W.X., He, S.G., An, J.B., Yang, F.M. and Dong, L. (2017). Influence of preparation methods on the physicochemical properties and catalytic performance of MnO_x-CeO_2 catalysts for NH_3-SCR at low temperature. *Chin. J. Catal.* 38: 146–159.

Yu, X.H., Li, J.M., Wei, Y.C. and Zhao, Z. (2014). Three-dimensionally ordered macroporous $Mn_xCe_{1-x}O_\delta$ and $Pt/Mn_{0.5}Ce_{0.5}O_\delta$ catalysts: Synthesis and catalytic performance for soot oxidation. *Ind. Eng. Chem. Res.* 53: 9653–9664.

Yu, X.N., Cao, F.F, Zhu, X.B., Zhu, X.C., Gao, X., Luo, Z.Y. and Cen, K.F. (2017). Selective catalytic reduction of NO over Cu–Mn/OMC catalysts: Effect of preparation method. *Aerosol Air Qual. Res.* 17: 302–313.

Zhu, Z.P., Liu, Z.Y., Niu, H.X., Liu, S.J., Hu, T.D., Liu, T. and Xie, Y.N. (2001). Mechanism of SO_2 promotion for NO reduction with NH_3 over activated carbon-supported vanadium oxide catalyst. *J. Catal*. 197: 6–16.

Received for review, October 28, 2019
Revised, December 31, 2019
Accepted, January 16, 2020